The Use of Equivalent Potential Vorticity to Diagnose Regions of Conditional Symmetric Instability

JAMES T. MOORE

Department of Earth and Atmospheric Sciences, Saint Louis University, St. Louis, Missouri

THOMAS E. LAMBERT

Seventh Weather Squadron/DON, APO AE, Heidelburg, AIN, Germany

(Manuscript received 7 August 1992, in final form 16 February 1993)

ABSTRACT

Conditional symmetric instability (CSI) is an important property of the atmosphere when diagnosing and predicting mesoscale bands of moderate to heavy precipitation within winter cyclones. Within regions of CSI, slantwise convection can increase snow totals over narrow regions. Typically, CSI is evaluated in a cross-sectional plane chosen normal to the middle-tropospheric thermal wind using M_g, the absolute geostrophic momentum, and θ_e, the equivalent potential temperature. Regions where M_g surfaces slope less than θ_e surfaces are subject to CSI. We describe an objective measure of CSI, called the equivalent potential vorticity (EPV), that makes evaluating CSI quick and effective. Cross sections of M_g versus θ_e and EPV are compared for two cases to demonstrate the effectiveness of using EPV cross sections to diagnose CSI. The distinction between slantwise convection and upright convection is also demonstrated by these case studies.

1. Introduction

The traditional Norwegian cyclone model displays an organized narrow line of showers associated with the cold front, and a broad shield of light, steady precipitation ahead of the warm front. However, numerous studies (e.g., Hobbs 1978; Houze et al. 1976; Shields et al. 1991; Byrd 1989) note the presence of mesoscale bands within a cyclone's precipitation areas. Mesoscale precipitation bands associated with winter cyclones can be the result of numerous processes, including gravity wave propagation within atmospheric ducts, boundary-layer convergence, frontogenetical forcing, frontal circulations, conditional symmetric instability (CSI), and vertical shear instability in the middle troposphere above cold frontal zones (Shields et al. 1991). In this paper we focus on diagnosing CSI using standard rawinsonde or model data.

CSI can result in slantwise convection over meso-β (20–200-km) scales of motion yielding substantially increased snow/rain totals over narrow bands. CSI has been thoroughly discussed by Bennetts and Hoskins (1979), Emanuel (1983a,b, 1985, 1988), Sanders and Bosart (1985), and, most recently, Snook (1992). The importance of CSI and frontogenetical forcing in winter storms in creating mesoscale heavy precipitation bands (sometimes accompanied by thunder) has been documented by Sanders and Bosart (1985), Sanders (1986), and Moore and Blakley (1988). Colman (1990a,b) has described synoptic environments in which the convective available potential energy (CAPE) is negligible, yet thunderstorms are supported above frontal surfaces (elevated convection) with cool boundary-layer temperatures. These elevated thunderstorms can also form heavy precipitation bands and are often near regions of CSI. Gyakum (1987) diagnosed CSI in the vicinity of heavy snow bands in an otherwise weak synoptic environment. Reuter and Yau (1990) related CSI to the presence of multiple bands of precipitation during the Canadian Atlantic Storms Program (CASP). Most recently, Martin et al. (1992) studied a rainband of moderate intensity over the eastern Carolinas on 26 January 1986. They concluded that the rainband formed in the updraft portion of a thermally direct vertical circulation in the vicinity of an upper-level frontal zone in an area of CSI. Typically, the precipitation band associated with CSI is oriented parallel to the vertical wind shear (or thickness), has a width on the order of tens of kilometers to around 100 km, and has a component of motion toward the warm air (Shields et al. 1991).

Bennetts and Hoskins (1979), Emanuel (1983), Martin et al. (1992), and Shields et al. (1991) note that CSI can be diagnosed by computing a quantity called the equivalent potential vorticity (EPV). However, they do not show explicit fields demonstrating

Corresponding author address: Prof. James T. Moore, Department of Earth and Atmospheric Sciences, Saint Louis University, 3507 Laclede Avenue, St. Louis, MO 63103-2010.

the relationship between CSI and EPV. In section 2, we define CSI and EPV and discuss the relationship between them. In section 3, we show examples of EPV, and illustrate its utility in diagnosing CSI and the potential for moderate to heavy precipitation bands forming within precipitation shields attendant to cyclones. We demonstrate that EPV is an easy and objective method for evaluating CSI, and also show how to distinguish cases of CSI from those of upright convection in the cold air ahead of a frontal zone.

2. CSI and EPV

As described by Sanders and Bosart (1985) and Moore and Blakley (1988), CSI in a near-saturated atmosphere can be evaluated in a cross section taken normal to the midtropospheric thermal wind by displaying lines of constant M_g and θ_e, the equivalent potential temperature. Emanuel (1983a) defines M_g as the absolute geostrophic momentum, which is equal to $V_g + fx$, where V_g is the geostrophic wind component normal to the cross section, f is the Coriolis parameter, and x is the distance from the left-hand side of the cross section in meters, increasing toward the warm air.

To produce the required fields of M_g and θ_e we used objectively analyzed fields of θ_e, u_g, and v_g (geostrophic wind components) at 17 levels, from 900 to 100 mb in 50-mb increments on a 31-column by 23-row grid covering the United States (grid distance of 190.5 km). Upon choosing a northern and southern point for the cross section, taken normal to the 850–300-mb thickness, values of θ_e and the geostrophic wind component normal to the cross section were interpolated to the line of the cross section. In the x–z plane of the cross section the result is a 20 (x axis) by 21 (z axis) grid of M_g and θ_e, where x equals 0 at the northernmost point and increases toward the warm air.

CSI can be evaluated by qualitatively comparing the slope of the θ_e surfaces with the slope of the M_g surfaces. CSI is diagnosed in these regions where the M_g surfaces are "flatter" (more horizontal) than the θ_e surfaces. It can be shown that in those regions a parcel is stable with respect to purely vertical or horizontal motions (i.e., buoyantly and inertially stable) but is conditionally unstable with respect to slantwise motions. For CSI to be an important consideration, the relative humidities should exceed 80% in the region (Bennetts and Sharp 1982).

Bluestein (1986) notes that CSI is favored under the following conditions: large vertical wind shear, large anticyclonic wind shear, and low static stability. In areas of large vertical wind shear, M_g surfaces will be relatively horizontal since V_g increases with height. When anticyclonic wind shear is present, the absolute vorticity will approach zero, creating a weak inertially stable zone, which may contribute to CSI. Finally, in regions of low static stability, isentropic (and likely θ_e) surfaces will be close to vertical. Understanding these factors helps one to see how EPV can be used to evaluate CSI.

Bennetts and Hoskins (1979) first discussed the wet-bulb potential vorticity based on the wet-bulb potential temperature. Emanuel (1983) later described an EPV based on the equivalent potential temperature. However, Martin et al. (1992) quantitatively defined the EPV as

$$\text{EPV} = -\boldsymbol{\eta} \cdot \nabla \theta_e, \tag{1}$$

where $\boldsymbol{\eta}$ is the three-dimensional vorticity vector; ∇ is the gradient del operator in x, y, and p coordinates; and θ_e is the equivalent potential temperature. Expanding (1), assuming geostrophic flow, neglecting terms with ω (vertical motion in pressure coordinates), neglecting terms involving variations with respect to y, and multiplying by g (gravitational acceleration) results in

$$\text{EPV} = g[(\partial M_g/\partial p \, \partial \theta_e/\partial x) - (\partial M_g/\partial x \, \partial \theta_e/\partial p)] \tag{2}$$

Terms: A B C D

Term 1 = Term A × Term B

Term 2 = Term C × Term D,

where $g = 9.806 \text{ m s}^{-2}$. The equation is multiplied by g so that the units of EPV will be the same as potential vorticity units (PVU) in Système International notation, where $1 \text{ PVU} = 1 \times 10^{-6} \text{ m}^2 \text{ K s}^{-1} \text{ kg}^{-1}$. EPV can be used to determine if CSI exists in an area (Martin et al. 1992). If EPV < 0 and the atmosphere is convectively stable, the atmosphere is conditionally symmetrically unstable, and when EPV > 0, the atmosphere is symmetrically stable. Snook (1992) notes that the computation of EPV (or moist PV) will determine the potential for CSI regardless of the directional shear of the actual geostrophic wind. Essentially, the criterion to satisfy CSI (EPV < 0) requires the absolute vorticity to be negative on a θ_e surface. A term by term explanation of (2) will help explain the relationship between EPV and CSI. Term 1 is defined as the product of term A and term B, and term 2 is defined as the product of term C and term D.

Term A represents the change in absolute geostrophic momentum with respect to pressure and is generally negative below the level of the jet stream. By definition, $M_g = V_g + fx$. Thus, M is directly proportional to V_g, and under normal atmospheric conditions, V_g increases as pressure decreases up to the jet stream level, which is required by the orientation of the cross section. It follows that term A will be less than 0 below the jet stream under these conditions. As the vertical wind shear increases, due to increasing V_g with height, term A will become smaller (more negative) and the slope of the M_g surfaces will decrease (M_g surfaces become more horizontal). This increases the opportunity for CSI in the region of fronts, where the slope of

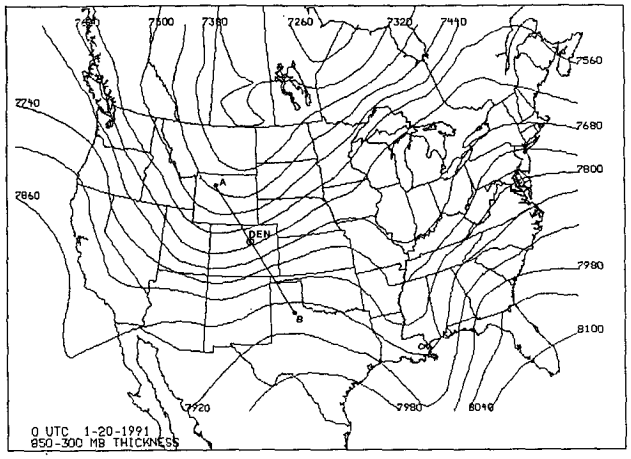

FIG. 1. The 850–300-mb thickness (gpm) for 0000 UTC 20 January 1991. Line A–B depicts the position of cross section shown in Figs. 3–6. DEN = Denver's Stapelton International Airport, Colorado.

equivalent potential temperature surfaces tends to be steep.

Term B is generally positive as a result of the definition of M_g, which requires that the cross section be taken normal to the geostrophic wind. Hence, the cross section is also normal to the 850–300-mb thickness pattern or thermal wind. Since the positive x direction on these sections points toward warmer air, equivalent potential temperature surfaces slope down and term B will be greater than 0. Therefore, the net result of term A multiplied by term B will be a negative number made more negative by a stronger horizontal θ_e gradient or vertical wind shear.

The value of term C is usually greater than 0, for several reasons. Since $M_g = V_g + fx$, $\partial M_g/\partial x$ is the absolute geostrophic vorticity (since u_g is $\simeq 0$). The absolute vorticity is usually greater than 0 in the Northern Hemisphere. An exception would result from a very strong decrease in V_g in the positive x direction. This effect could overpower the increase in M_g due to fx and cause term C to become negative. In most cases, the gradient of V_g in the x direction will not be large enough to cause term C to be less than 0.

Term D is a measure of the convective stability of the atmosphere. If term D is less than 0, the atmosphere is convectively stable. If term D equals 0, the atmosphere is convectively neutral, and if term D is positive, the atmosphere is convectively unstable. The effect of term D on the value of EPV is now evaluated for each of the foregoing three alternatives. In each case, term 1 (term A multiplied by term B) is assumed to be negative, and term C is assumed to be positive; this is usually true. Under these conditions, there are three possibilities.

Case 1: Term D < 0, the atmosphere is convectively stable, making term 2 negative. When term 2 is subtracted from term 1 in (2), the net result is to increase the value of EPV and decrease chances for CSI.

Case 2: Term D = 0, the atmosphere is convectively neutral. This results in term 2 = 0; as a result term 2 does not affect the overall value of EPV.

Case 3: Term D > 0, the atmosphere is potentially convectively unstable. In this case, upright convection will result in a moist atmosphere from upward vertical motion, and the diagnosis of CSI is a moot point. Bennetts and Sharp (1982) note that the atmosphere can be unstable to both CSI and convective instability. However, since convection has a faster growth rate, it predominates. They note that it is necessary to differentiate between frontal regions unstable to CSI and areas of potential instability released through convection.

Evaluating terms 1 and 2 reveals, as noted by Bennetts and Hoskins (1979), that the equivalent potential vorticity must be negative for CSI to exist in a convectively stable atmosphere. The release of CSI requires a near-saturated environment with a lifting mechanism, typically (but not exclusively) diagnosed in the vicinity of a warm frontal zone.

3. Case studies documenting CSI and EPV

To document the utility of EPV to diagnose CSI, we now show two case studies of heavy snow events: one from 20 January 1991, and the other from 15 December 1987. Our goal in this paper is not to present ex-

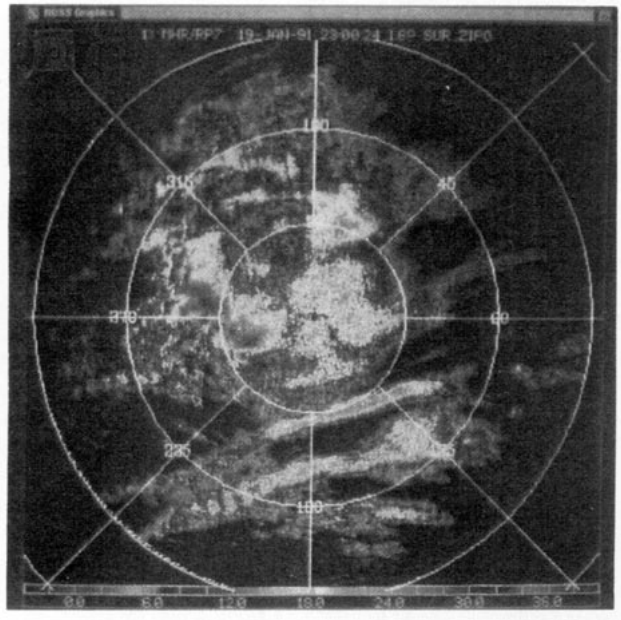

FIG. 2. Plan position indicator at 1.6° elevation angle from the Mile-High radar on 2300 UTC 19 January 1991. Reflectivity (in dBZ) is indicated by the bar along the bottom of the figure. Range rings are at 50 km (Rasmussen et al. 1992).

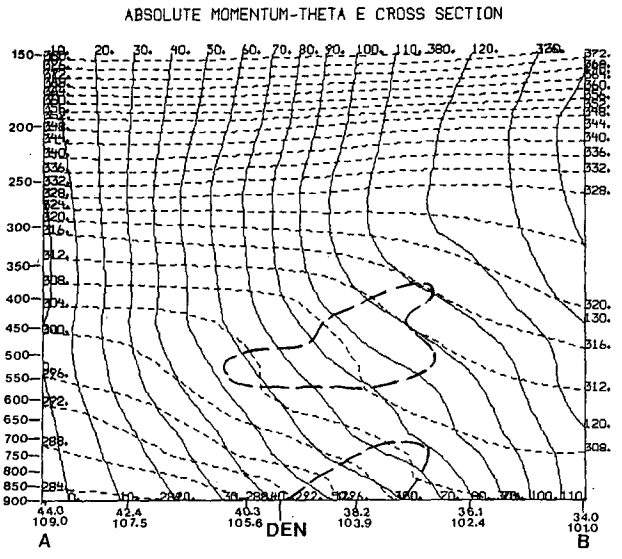

FIG. 3. Vertical cross section of absolute geostrophic momentum (Mg, solid lines) and equivalent potential temperature (θ_e, dashed lines) along line A–B (see Fig. 1) for 0000 UTC 20 January 1991. Outlined area denotes region of CSI. Location of Denver's Stapelton International Airport is noted along the x axis as DEN. Latitude and longitude of points along the cross section are displayed along the x axis.

haustive case studies of these storms but to demonstrate how CSI and EPV can be used to estimate those regions that might experience heavier snowfall than might otherwise be expected.

Figure 1 shows the 850–300-mb thickness for 0000 UTC 20 January 1991. A cross section was taken normal to the thickness lines (and therefore the thermal wind) along line A–B to diagnose CSI. This particular

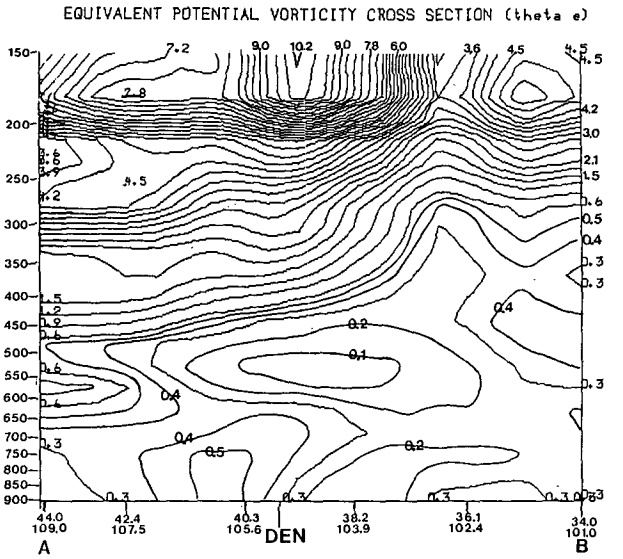

FIG. 5. Vertical cross section of term 2 of EPV (including $-g$ factor) [see (2)] in PVU (1×10^{-6} m^2 K s^{-1} kg^{-1}) along line A–B (see Fig. 1) for 0000 UTC 20 January 1991.

line was chosen since the Mile-High radar at Denver, Colorado, at 2300 UTC 19 January 1991 reported well-defined precipitation bands with reflectivities up to 32 dBZ (Fig. 2). Snow began falling around 1800 UTC 19 January and lasted about 18 h, resulting in snow depths from 2.5 to 12 cm (1 to 4.7 in.) near Denver (Rasmussen et al. 1992). Rasmussen et al. (1992) note that echo tops were approximately 6.8 km MSL, with the long axis of the precipitation bands oriented parallel to the upper-air flow.

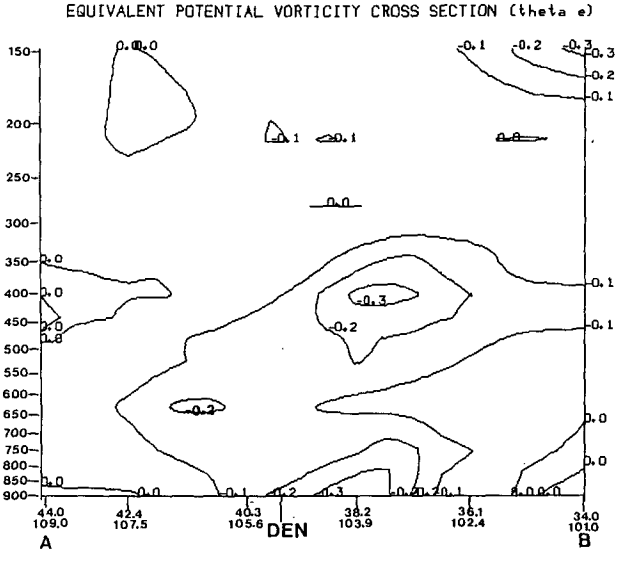

FIG. 4. Vertical cross section of term 1 of EPV [see (2)] in PVU (1×10^{-6} m^2 K s^{-1} kg^{-1}) along line A–B (see Fig. 1) for 0000 UTC 20 January 1991.

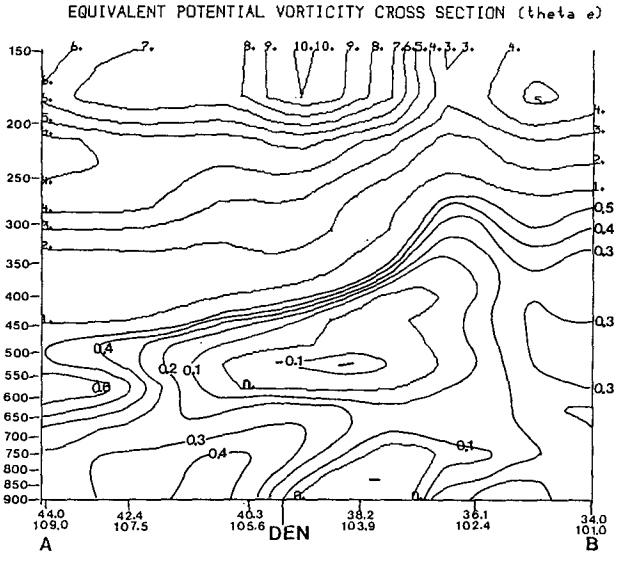

FIG. 6. Vertical cross section of EPV in PVU (1×10^{-6} m^2 K s^{-1} kg^{-1}) along line A–B (see Fig. 1) for 0000 UTC 20 January 1991. Negative region depicts CSI.

A cross section of θ_e and M_g along line A–B is shown in Fig. 3. The outlined areas denote where the θ_e surfaces are slightly more vertical than the M_g surfaces. It is important to note, however, that although a small region gets close to being convectively neutral, there is no evidence of convective instability in this cross section.

Figure 4 reveals term 1 in (2). As discussed in section 2, this term tends to be negative. Indeed, the most negative region shows up where the M_g surfaces are sloped from lower right to upper left at about a 45° angle. Figure 5 displays term 2 (including the $-g$ factor) for the same time. Note that there are no negative areas that would indicate convective instability. Thus, in a convectively stable atmosphere, term 2 can "contribute" to CSI by becoming nearly zero without becoming convectively unstable (i.e., θ_e surfaces "folding" over themselves).

Finally, Fig. 6 shows the total EPV for the same cross section. Two areas of EPV < 0 are diagnosed: one along the surface, and a larger one aloft (from ~600 to 450 mb) over the Denver area. An examination of the Denver sounding (not shown) reveals that the average relative humidity from the surface to 450 mb is about 80%, with higher values (>90%) from the surface to 700 mb. This would meet the relative humidity criterion for a CSI region. CSI in this region would help explain the multiple banded precipitation pattern near the Mile-High radar.

The next case is a good example of how one must discriminate between regions of CSI and convective instability. As noted earlier, CSI and convective instability may coexist, but due to its faster growth rate, convective instability will dominate CSI, generating shorter temporal- and spatial-scale features.

Figure 7 shows the 850–300-mb thickness for 0000 UTC 15 December 1987. A cross section was taken normal to the thickness lines along line C–D to diagnose CSI. This particular line was chosen since several stations in the vicinity (JLN = Joplin, Missouri; SGF = Springfield, Missouri; and HRO = Harrison, Arkansas) reported thunder and frozen precipitation at or around 0000 UTC. Also, as shown in Fig. 8, snowfall reports in Missouri revealed a banded structure, especially in west-central and southwestern Missouri.

A cross section of θ_e and M_g along line C–D in Fig.

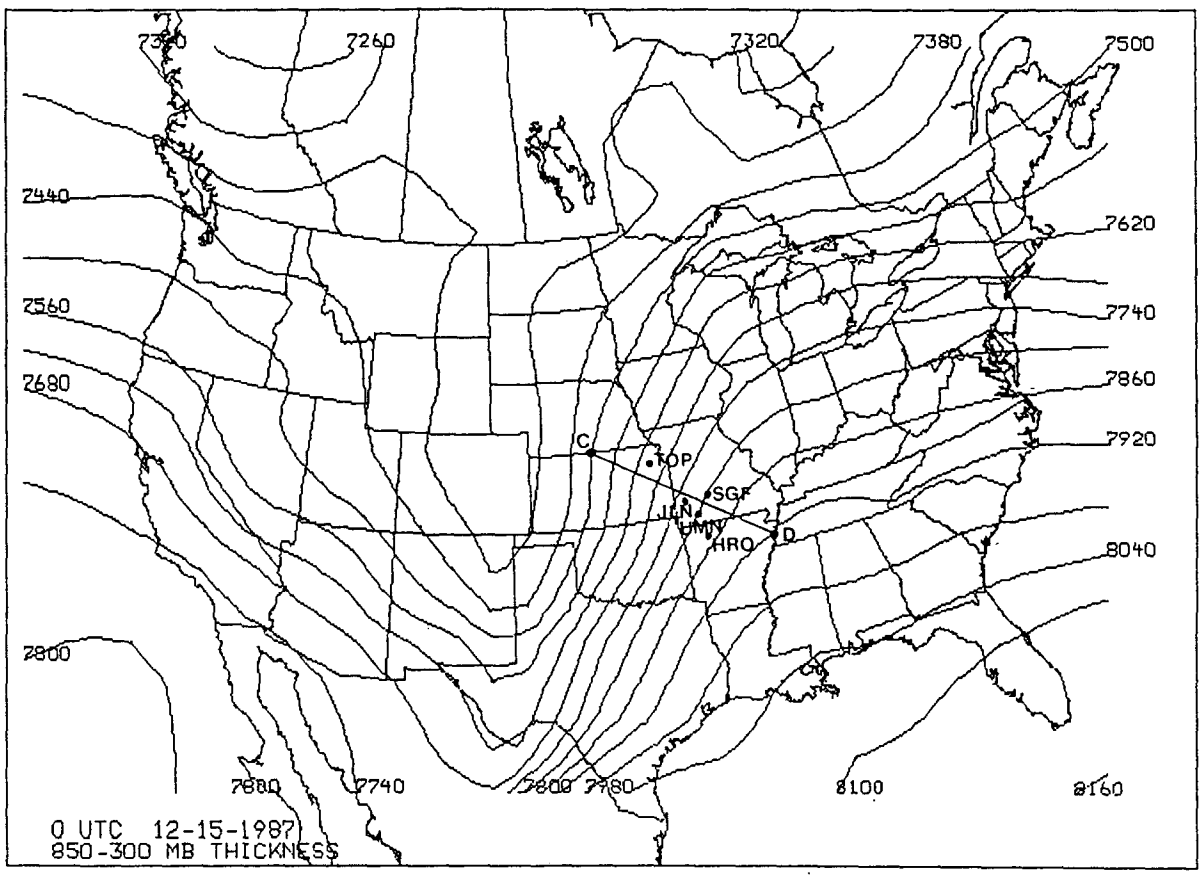

FIG. 7. The 850–300-mb thickness (gpm) for 0000 UTC 15 December 1987. Three-letter station identifiers at filled circles are JLN = Joplin, Missouri; SGF = Springfield, Missouri; HRO = Harrison, Arkansas; TOP = Topeka, Kansas; and UMN = Monett, Missouri. JLN, SGF, and HRO reported thunder and frozen precipitation at or around 0000 UTC. Line C–D depicts the position of the cross section shown in Figs. 9–12.

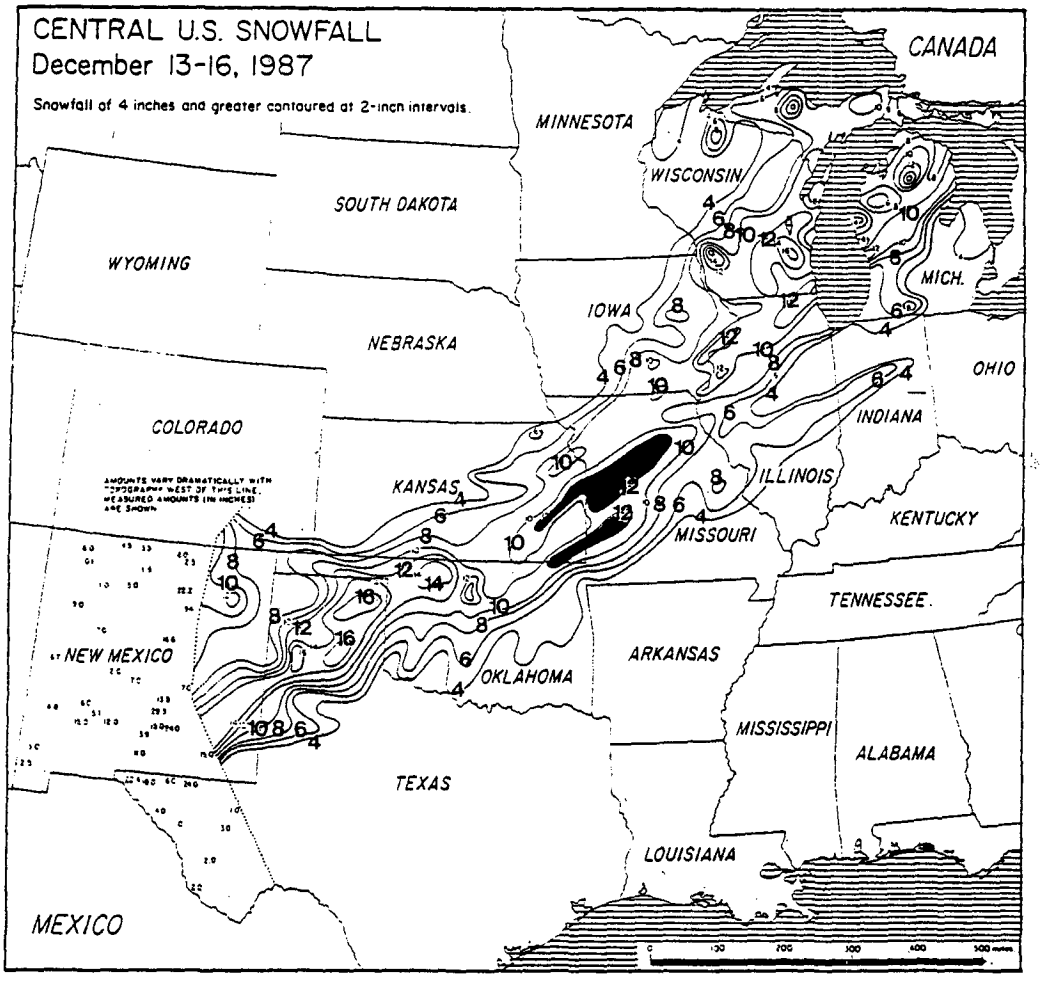

FIG. 8. Total storm snowfall for 13–16 December 1987. Note banded 12-in. isopleths (blackened areas) in west-central and southwest Missouri (NCDC 1987).

7 is shown in Fig. 9. Note that there is a large region where the θ_e isopleths are nearly vertical or fold over themselves. The latter folded regions are regions of convective instability created from warm, moist air riding over a warm frontal boundary. Areas with cold boundary-layer temperatures (low θ_e values) with convective instability *aloft* are susceptible to elevated convection given upward vertical motion and near-saturated conditions. Colman (1990a,b) has also examined elevated thunderstorms in regions with *no* positive CAPE and *no* convective instability. In these cases, elevated thunderstorms were the result of frontogenetical forcing in the presence of *weak* symmetric *stability*. The outlined area depicts the CSI region, including the convectively unstable zone. Term 1 of (2) is shown in Fig. 10 and reveals mostly negative values, with a large negative area extending upward and to the left. Term 2 along the same cross section (Fig. 11) displays mostly positive values, with the exception of a larger negative region sloping northward along the warm frontal zone. This negative region denotes convective instability, since term 2 will be less than 0 only in convectively unstable zones. In this region, upright convection is favored over slantwise convection due to a greater growth rate. An examination of the soundings from both Monett, Missouri (UMN), and Topeka, Kansas (TOP), reveals that the mean relative humidity exceeded 85% in the surface to 540-mb layer at this time. Therefore, regions north of the warm front will likely experience elevated convection.

Finally, Fig. 12 shows the total EPV field for the cross section along line C–D. On this figure the convectively unstable region is stippled to show that this is a region favoring elevated upright convection and not CSI. However, it is possible that the elevated upright convection was organized and modified by the slantwise convection, since the snowfall totals do reveal a banded structure. The only area of CSI is shown between 350 and 400 mb to the north. Since this area is relatively shallow and quite high in the troposphere (where the relative humidity is lower and vertical motions are likely weaker), it is unlikely to contribute to

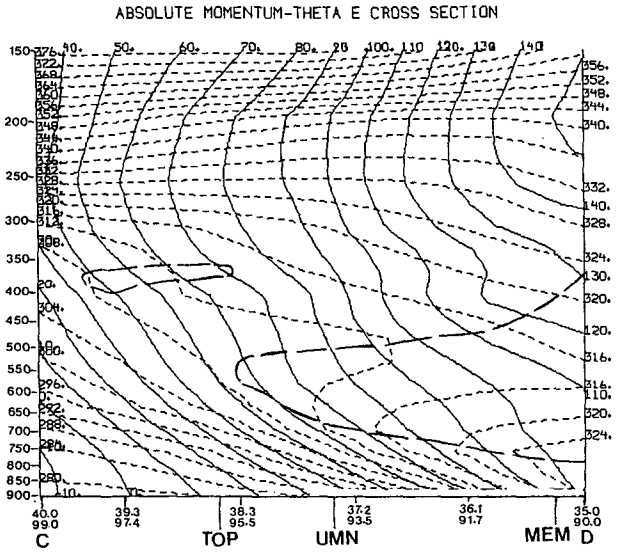

FIG. 9. Same as Fig. 3 except for 0000 UTC 15 December 1987 along line C–D (see Fig. 7). Reference stations on x axis are TOP = Topeka, Kansas; UMN = Monett, Missouri; and MEM = Memphis, Tennessee. Outlined area denotes region of CSI (includes convectively unstable region).

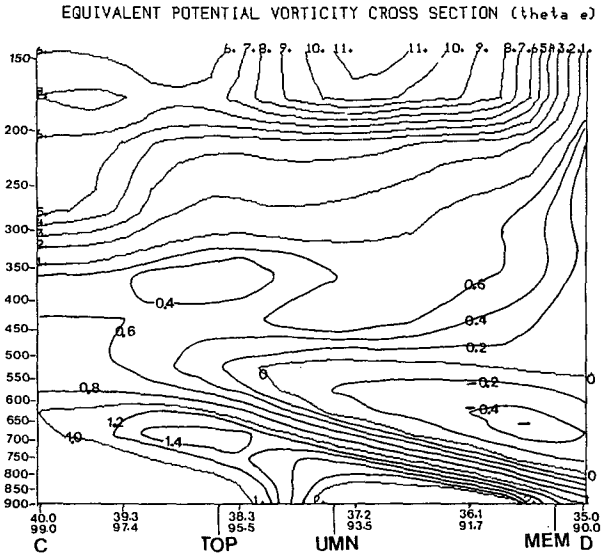

FIG. 11. Same as Fig. 5 except for 0000 UTC 15 December 1987 along line C–D (see Fig. 7).

precipitation. This case demonstrates that EPV is a useful parameter to diagnose CSI, but it should be used with care since CSI can coexist with convective instability and the latter typically dominates.

4. Conclusions

It has been shown that the subjective method of diagnosing CSI using cross sections of θ_e and M_g can be replaced by computing EPV within the cross sectional plane. Values where EPV < 0 in a convectively stable atmosphere are regions of CSI. EPV, evaluated by comparing derivatives of M_g and θ_e in the vertical and along the cross-sectional plane, effectively diagnoses those regions where the absolute geostrophic momentum surfaces slope less than the θ_e surfaces. Given sufficient moisture and upward vertical motion, regions of CSI can result in heavy precipitation bands that tend to be oriented parallel to the thickness field.

However, since CSI and convective instability can coexist, it is useful to examine both terms comprising EPV to diagnose convectively unstable regions (where term 2 < 0). Term 1, involving the horizontal com-

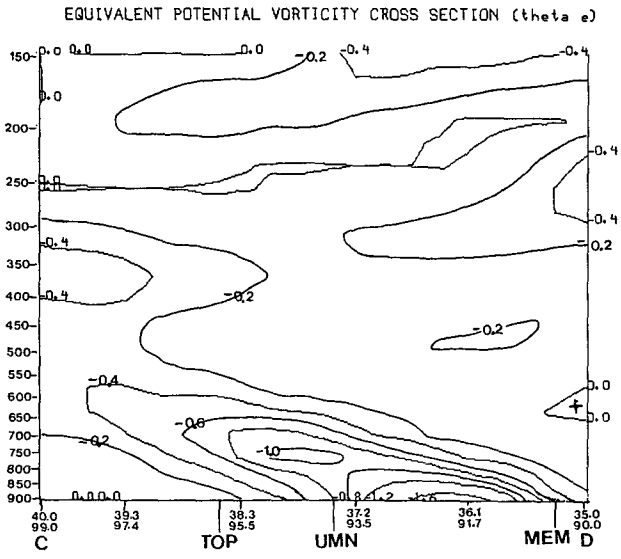

FIG. 10. Same as Fig. 4 except for 0000 UTC 15 December 1987 along line C–D (see Fig. 7).

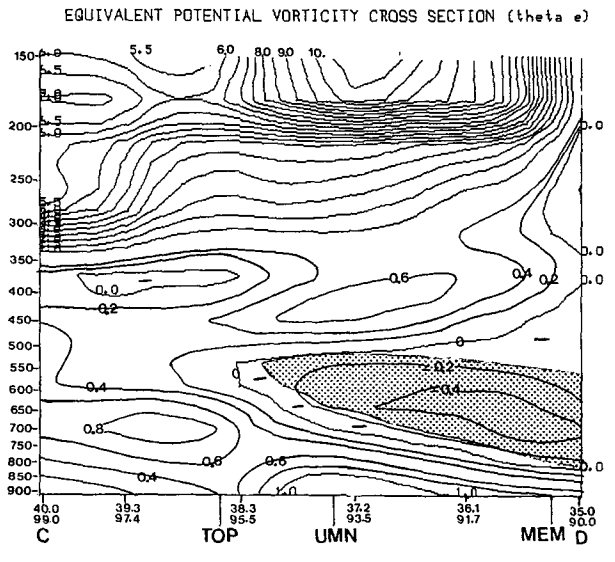

FIG. 12. Same as Fig. 6 except for 0000 UTC 15 December 1987 along line C–D (see Fig. 7). Stippled region depicts region of convective instability. Negative sign depicts region of CSI.

ponent of geostrophic vorticity and the horizontal θ_e gradient, is equally as important in the lower troposphere as term 2, which is the traditional simplification of potential vorticity. Thus, computing only the potential vorticity could be misleading in some situations. In convectively unstable regions, upright convection will dominate over slantwise convection, often creating elevated convection.

In convectively stable regions, it is still possible to have elevated convection given sufficient frontogenetical forcing in a region of weak symmetric stability. An EPV diagnosis can identify either case. The concept of EPV is useful in understanding how CSI is created. Using EPV to estimate regions of CSI is quick and objective, and therefore, has direct applicability to the operational community.

Acknowledgments. The authors would like to thank the Air Force Institute of Technology for providing the junior author with the opportunity to work toward his M.S. in meteorology at Saint Louis University, of which this paper is an outgrowth. The senior author wishes to acknowledge the support of the Cooperative Program for Meteorology, Education and Training (COMET), which funded this research. The authors would also like to thank the editor (Dr. Brad Colman) and the two anonymous reviewers for their critically constructive reviews. Finally, Ms. Jeanne Mueller is appreciated for her expert typing of the manuscript.

REFERENCES

Bennetts, D. A., and B. J. Hoskins, 1979: Conditional symmetric instability—A possible explanation for frontal rainbands. *Quart. J. Roy. Meteor. Soc.*, **105,** 945–962.

——, and J. D. Sharp, 1982: The relevance of conditional symmetric instability to the prediction of mesoscale frontal rainbands. *Quart. J. Roy. Meteor. Soc.*, **108,** 595–602.

Bluestein, H., 1986: Fronts and jet streaks: A theoretical perspective. *Mesoscale Meteorology and Forecasting,* Peter Ray, Ed., Amer. Meteor. Soc., 173–215.

Byrd, G. P., 1989: A composite analysis of winter season overrunning precipitation bands over the Southern Plains of the United States. *J. Atmos. Sci.*, **46,** 1119–1132.

Colman, B. R., 1990a: Thunderstorms above frontal surfaces in environments without positive CAPE. Part I: A climatology. *Mon. Wea. Rev.*, **118,** 1103–1121.

——, 1990b: Thunderstorm above frontal surface in environments without positive CAPE. Part II: Organization and instability mechanisms. *Mon. Wea. Rev.*, **118,** 1123–1144.

Emanuel, K. A., 1983a: The Lagrangian parcel dynamics of moist symmetric instability. *J. Atmos. Sci.*, **40,** 2368–2376.

——, 1983b: On assessing local conditional symmetric instability from atmospheric soundings. *Mon. Wea. Rev.*, **111,** 2016–2033.

——, 1985: Frontal circulations in the presence of small moist symmetric stability. *J. Atmos. Sci.*, **42,** 1062–1071.

——, 1988: Observational evidence of slantwise convective adjustment. *Mon. Wea. Rev.*, **116,** 1805–1816.

Gyakum, J. R., 1987: Evolution of a surprise snowfall in the United States Midwest. *Mon. Wea. Rev.*, **115,** 2322–2345.

Hobbs, P. V., 1987: Organization and structure of clouds and precipitation on the mesoscale and microscale in cyclonic storms. *Rev. Geophys. Space Physics,* **16,** 741–755.

Houze, R. A., P. V. Hobbs, K. R. Biswas, and W. M. Davis, 1976: Mesoscale rainbands in extratropical cyclones. *Mon. Wea. Rev.*, **104,** 868–878.

Martin, J. E., J. D. Locatelli, and P. V. Hobbs, 1992: Organization and structure of clouds and precipitation on the mid-Atlantic Coast of the United States. Part V: The role of an upper-level front in the generation of a rainband. *J. Atmos. Sci.*, **49,** 1293–1303.

Moore, J. T., and P. D. Blakley, 1988: The role of frontogenetical forcing and conditional symmetric instability in the Midwest snowstorm of 30–31 January 1982. *Mon. Wea. Rev.*, **116,** 2155–2171.

NCDC, 1987: National Climatic Data Center, NOAA, *Storm Data,* No. 29 (December), 44 p.

Rasmussen, R., M. Politovich, J. Marwitz, W. Sand, J. McGinley, J. Smart, R. Pielke, S. Rutledge, D. Wesley, G. Stossmeister, B. Bernstein, K. Elmore, N. Powell, E. Westwater, B. B. Stankov, and D. Burrows, 1992: Winter Icing and Storms Project (WISP). *Bull. Amer. Meteor. Soc.*, **73,** 951–974.

Reuter, G. W., and M. K. Yau, 1990: Observations of slantwise convective instability in winter cyclones. *Mon. Wea. Rev.*, **118,** 447–458.

Sanders, F., 1986: Frontogenesis and symmetric stability in a major New England snowstorm. *Mon. Wea. Rev.*, **114,** 1847–1862.

——, and L. F. Bosart, 1985: Mesoscale structure in the megalopolitan snowstorm of 11–12 February 1983. Part I: Frontogenetical forcing and symmetric instability. *J. Atmos. Sci.*, **42,** 1050–1061.

Shields, M. T., R. M. Rauber, and M. K. Ramamurthy, 1991: Dynamical forcing and mesoscale organization of precipitation bands in a Midwest winter cyclonic storm. *Mon. Wea. Rev.*, **119,** 936–964.

Snook, J. S., 1992: Current techniques for real-time evaluation of conditional symmetric instability. *Wea. Forecasting,* **7,** 430–439.